



Organic Chemistry Department  
Babes-Bolyai University  
Cluj-Napoca, 400028  
ROMANIA

# **Cryptands, Molecular Devices and Bioactive Sugar Derivatives: Design, Synthesis and Structural Analysis**

**-Monica Violeta Cîrcu-  
PhD Thesis Abstract**

**Scientific advisor:  
Prof. Dr. ION GROSU**

**Cluj-Napoca  
September 2011**

**Key Words:** Cryptands

Cage Molecules

Molecular Devices

1,3-dioxanic Building Block

Anancomeric Structures

Podands

Bioactive Sugar Derivatives

Anomeric Conformers

**Jury:**

<b>Scientific advisor</b>	Prof. Dr. Ion GROSU	Babes-Bolyai University, Cluj-Napoca, Romania
<b>President</b>	Conf. Dr. Majdik Cornelia	Babes-Bolyai University, Cluj-Napoca, Romania
<b>Reviewer</b>	Assoc. Prof. Thanasis Gimisis	University of Athens, Athens, Greece
<b>Reviewer</b>	D. R. Dr. Mihai Barboiu	Montpellier University, France
<b>Reviewer</b>	Prof. Dr. Cristian SILVESTRU	Babes-Bolyai University, Cluj-Napoca, Romania
<b>Reviewer</b>	Conf. Dr. Ileana Farcasanu	Bucharest University, Bucharest, Romania

**Cluj-Napoca  
September 2011**

## CONTENTS

INTRODUCTION.....	1
PART 1. CAGE MOLECULES .....	3
1.1. General Remarks.....	4
1.2. Synthetic Methodologies for Macocyclization Reactions.....	7
1.3. General Remarks on Cu-catalyzed Acetylenic couplings.....	9
1.4. General Remarks on "click" reactions.....	10
1.5. Results and Discussions.....	12
1.6. Conclusions.....	44
1.7. Experimental Part.....	45
1.7.1. General Indications.....	45
1.7.2. Synthesis of Compounds.....	46
PART 2. MOLECULAR DEVICES .....	69
2.1. General Remarks.....	70
2.2. Results and Discussions.....	75
2.3. Conclusions.....	82
2.4. Experimental Part.....	83
2.4.1. General Indications.....	83
2.4.2. Synthesis of Compounds.....	84
PART 3. BIOACTIVE SUGAR DERIVATIVES .....	90
3.1. General Remarks.....	91
3.2. Results and Discussions.....	93
3.3. Conclusions.....	110
3.4. Experimental Part.....	111
3.4.1. General Indications.....	111
3.4.2. Synthesis of Compounds.....	112



**PART 1. CAGE MOLECULES**

## 1.5. RESULTS AND DISCUSSIONS

Our aim was to accomplish the synthesis of  $C_3$  symmetric macrocyclic compounds. To obtain the expected macrocycles, one symmetrically trisubstituted building block was required, our strategy for the synthesis of cage molecules being illustrated in **Figure 2**. The building block consist in an aromatic 1,3,5-trisubstituted unit bearing 1,3-dioxanic rings that presents non planar conformation and favor the formation of  $\pi$ - $\pi$  stacking interactions with different organic guest molecules. 1,3-Dioxanic rings are outside (oriented in the same direction) and they allow a preorganization. The functionalization of the precursors is possible at  $C_2$  of the dioxanic ring.

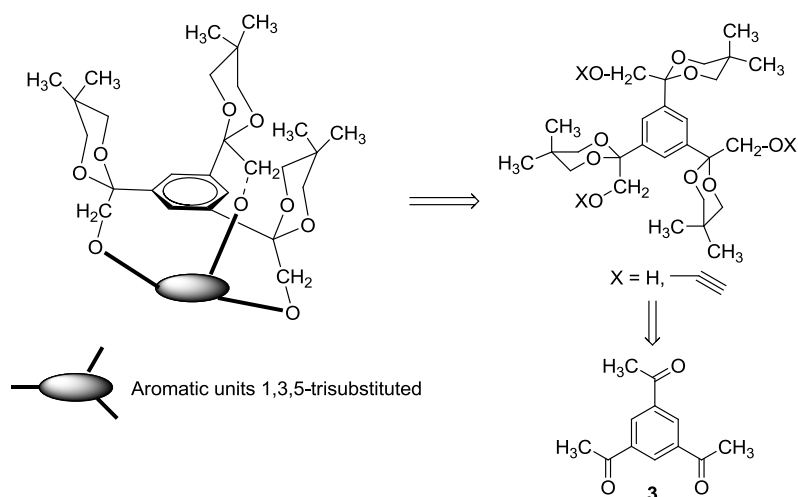
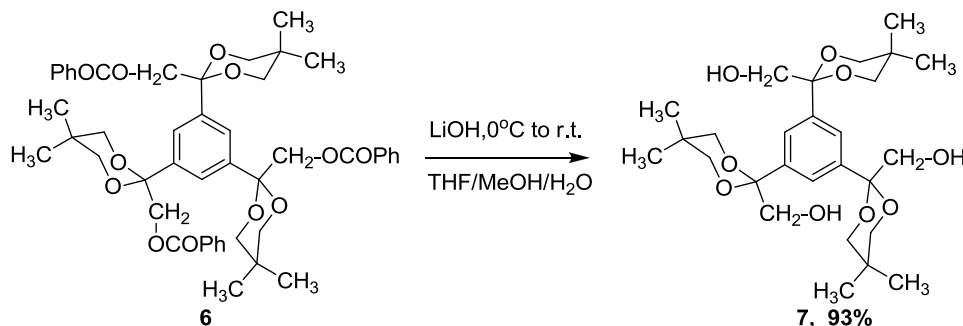


**Figure 2.** Retrosynthetic scheme for the new cage molecules.

The key intermediate **7** was obtained after a method adapted from a recently published procedure,<sup>1</sup> by deprotection of compound **6** with lithium hydroxide in a mixture of THF/MeOH/H<sub>2</sub>O at 0 °C (**Scheme 10**).



The structure of this compound **7** was investigated by NMR, MS and X-ray studies and appears to present anancomeric structure. The NMR spectra show different signals for axial and equatorial protons of 1,3-dioxanic cycles and also for protons and carbon atoms of axial and equatorial substituent in position 5. <sup>1</sup>H NMR spectrum (**Figure 5**) exhibit one characteristic AB system for the protons of 1,3-dioxanic cycles ( $\delta_{4,6 \text{ ax}} = 3.40 \text{ ppm}$ ;  $\delta_{4,6 \text{ eq}} = 3.48 \text{ ppm}$ ), one singlet for protons of group CH<sub>2</sub> in position 2', 2'' et 2''' ( $\delta = 3.56 \text{ ppm}$ ) and one singlet for the aromatic protons ( $\delta = 7.49 \text{ ppm}$ ). Both methyl groups in position 5' (5'' and 5''') present one singlet for the axial protons ( $\delta_{\text{CH}_3\text{ax}} = 1.29 \text{ ppm}$ ) and one singlet for the equatorial protons ( $\delta_{\text{CH}_3\text{eq}} = 0.62 \text{ ppm}$ ).

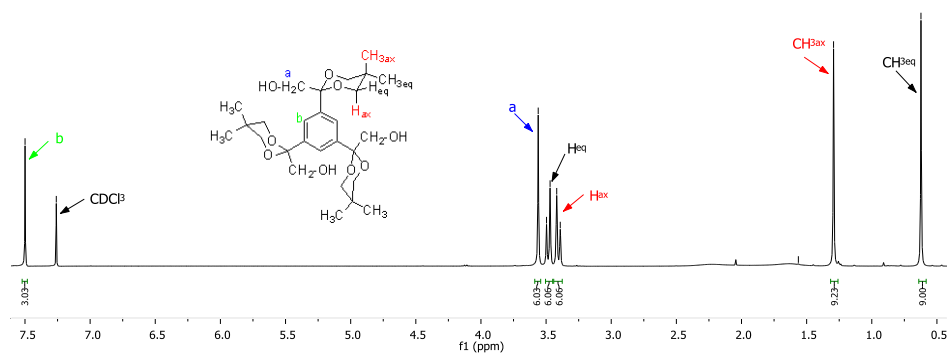


**Figure 5.** <sup>1</sup>H NMR spectrum (300 MHz, CDCl<sub>3</sub>) of compound **7**

<sup>1</sup> Florian, M.C.; Cîrcu, M.; Toupet, L.; Terec, A.; Grosu, I.; Ramondenc, Y.; Dinca, N.; Ple, G., *Cent. Eur. J. Chem.*, **2006**, *4* (4), 808-821.

The molecular structure (**Figure 7**) of triol **7**<sup>2</sup> reveals a conformer in which the aromatic group is axial for all 1,3-dioxane rings. The axial orientation of the aromatic unit is not surprising, in many previous works it was shown that in 2-methyl-2-aryl-1,3-dioxanes (or related heteroaromatic compounds) the larger methyl group prefers the equatorial position. Two of the 1,3-dioxane units are oriented on the same side of the plane of the aromatic ring, while the third heterocycle is disposed on the opposite side. The aromatic hydrogen atoms exhibit intramolecular contacts with the oxygen atoms of the 1,3-dioxane unit [ $d_{C(ar)-H\cdots O} = 2.488 - 2.564$ ]. The axial methyl groups located at positions 5 adopt H inside conformations and the inside H atoms exhibit bifurcated contacts with the oxygen atoms of the heterocycles [ $d_{C(sp^3)-H\cdots O} = 2.557 - 2.688$ ]. Other  $C(sp^3)-H\cdots O$  intramolecular contacts could be observed between H atoms of the  $CH_2$  groups and the oxygen atoms of the heterocycle [ $d_{C(sp^3)-H\cdots O} = 2.405 - 2.526$ ].

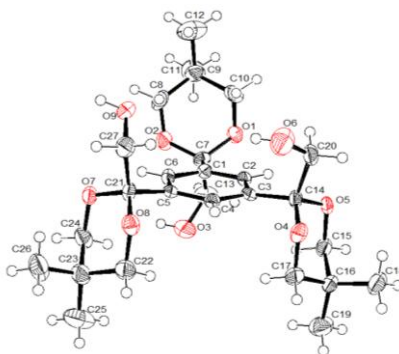


**Figure 7.** ORTEP diagram of compound **7**

In the lattice (view along the *a* axis) the podand forms layers (**Figure 8**). The aromatic rings can be considered all parallel (the angles between their planes are  $0^\circ$  or  $4.58^\circ$ ) and an alternation (head to tail arrangement) of the molecules with two 1,3-dioxane units oriented in one side and of those with two 1,3-dioxane units oriented in opposite side could be observed (**Figure 8**). Intermolecular hydrofobic contacts were observed between the H atoms of axial methyl groups at the positions 5 ( $d_{H\cdots H} = 2.326$  and  $2.392$  Å), and between H atoms of equatorial methyl groups and axial H atoms at positions 4 of the heterocycle ( $d_{H\cdots H} = 2.387$  Å).

<sup>2</sup> Cîrcu, M.; Pascanu, V.; Soran, A.; Braun, B.; Terec, A.; Socaci, C.; Grosu, I., *CrystEngComm.*, submitted.

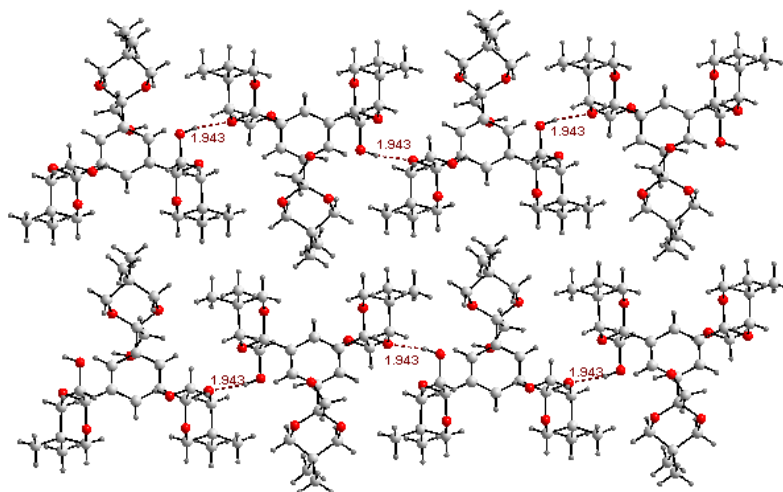
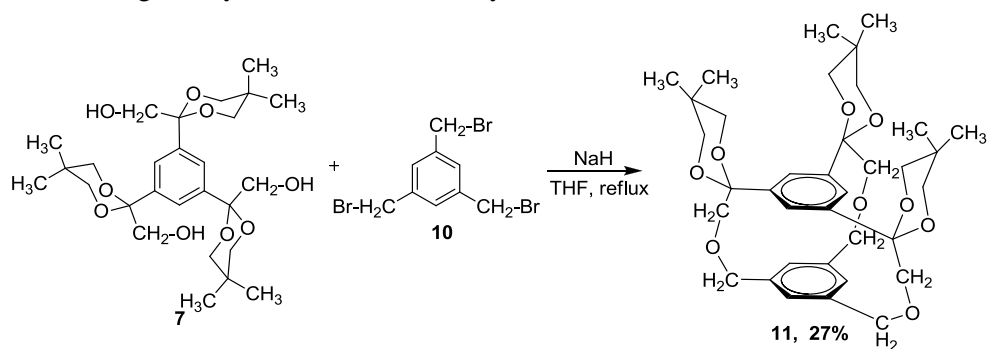


**Figure 8.** Diamond representation of the lattice showing the head-to-tail orientation of the molecules

Having two of the key compounds (**7** and **10**) in our hands we moved on to synthesize the molecular cage **11** conforming to **Scheme 12**. The macrocyclization reaction was performed in anhydrous THF in the presence of sodium hydride as a base and following the high dilution technique. The yield of the reaction is fair if we compare it with the literature for this type of reactions. The new molecular cage was investigated by NMR, MS and X-Ray studies.



**Scheme 12**

In the aliphatic region of proton NMR spectrum (**Figure 10**) of this compound we observe two different singlet signals corresponding to the protons from methyl groups in position 5 of the 1,3-dioxanic ring, one axial and one equatorial. We have also the AB system which is specific to the protons of position 4 and 6 from the 1,3-dioxanic ring (3.19 ppm for  $H_{4ax}$  and  $H_{6ax}$ , 3.36 ppm for  $H_{4eq}$  and  $H_{6eq}$

respectively). Two more singlet signals appear at 3.81 ppm and 4.24 ppm corresponding each to the protons from methylenic groups that are connecting the aromatic cycles together. In the aromatic area we observe two different singlets that correspond to the protons of the two benzene units of the molecule.

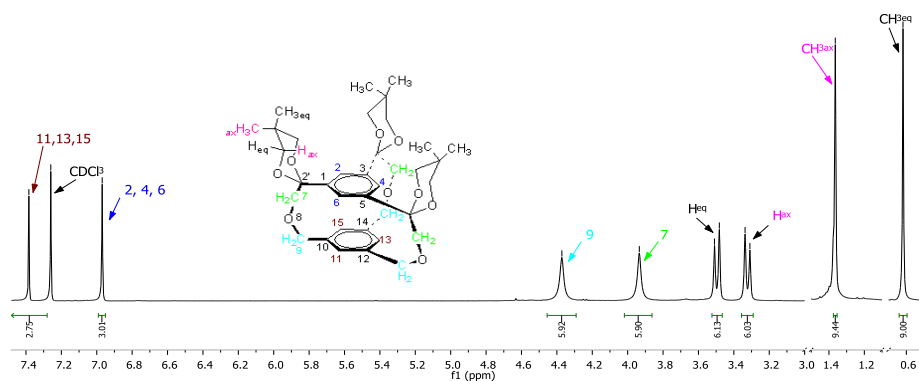


**Figure 10.**  $^1\text{H}$  NMR spectrum (300 MHz,  $\text{CDCl}_3$ ) of compound **11**

The molecular structure (**Figure 13**) of compound **11** reveals a molecule in which the aromatic group are axial for all 1,3-dioxane rings. Also it can be observed that all the 1,3-dioxane units are oriented on the same side with respect to the plane of the aromatic ring.

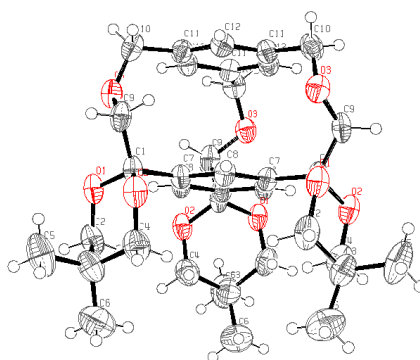


**Figure 13.** ORTEP diagram of compound **11**

In the lattice (view along the  $a$  axis **Figure 14**) the molecular cage forms layers. An alternation (tail to tail arrangement) of the molecules can be observed in the lattice, in one molecule the 1,3-dioxanic units are oriented in one direction while in the next molecule they are oriented in the opposite direction with respect to the aromatic units. We can as well observe from the lattice the molecules of

chloroform which are forming stacking with the aromatic units that are not bearing 1,3-dioxanic units.

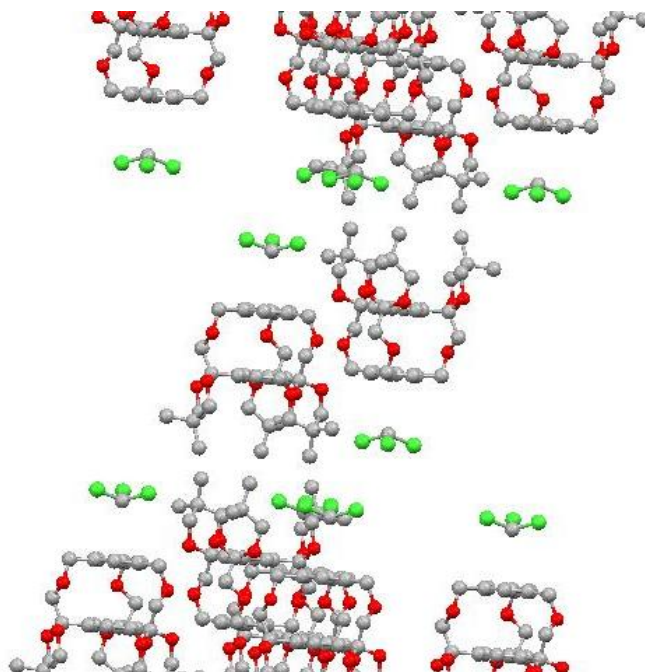


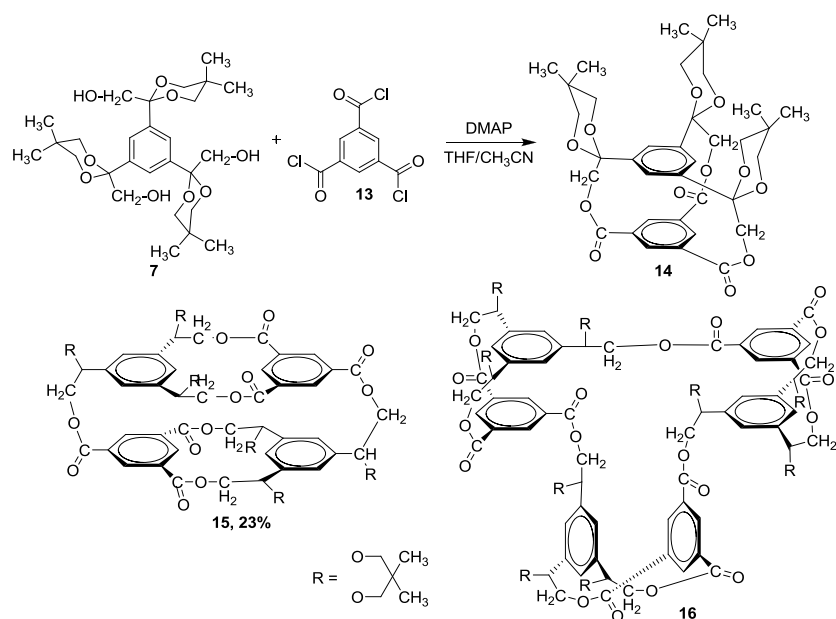
**Figure 14.** Mercury representation of the lattice showing the tail-to-tail orientation of the molecule

Another cage molecule designed is presented in **Scheme 14**. The macrocyclisation reaction was performed using a classic procedure described in the literature for synthesizing macrocyclic esters.<sup>3,4</sup> The crude of this reaction contained a mixture of monomer (**14**), dimer (**15**) and trimer (**16**). The major product of this reaction is the dimer **15**, which we were able to isolate and characterize by means of NMR and MS spectra. Due to the fact that the monomer and the trimer were in very small quantities we could not isolate and analyze them, but we could separate and observe them in HPLC-MS.

---

<sup>3</sup> Cao, J.; Fyfe, M.C., T.; Stoddart, J.F.; Cousins, G.R., L.; Glink, P.T., *J. Org. Chem.*, **2000**, *65*, 1937.

<sup>4</sup> Godbert, N.; Batsanov, A.S.; Bryce, M.R.; Howard, J.A.K., *J. Org. Chem.*, **2001**, *66*, 713.



Scheme 14

In the proton NMR of compound 15 (Figure 16) we observe the two singlet signals corresponding to the axial and equatorial protons of the methyl groups in position 5 of the 1,3-dioxane rings as we expected, but we can also observe another two singlet signals, of lower intensity. This brings us to the conclusion that four of the six 1,3-dioxane rings of the molecule are oriented outside of the molecule's cavity, while the other two are oriented to the inside of the molecule's cavity. Our theory is confirmed by the picks corresponding to the protons 4 and 6 of the 1,3-dioxane ring. We have here a set of AB systems instead of a single AB system that is specific to this type of compounds. Also in the aromatic area we can see the same distribution of signals, all this proving that indeed four of the dioxane rings are oriented in the same direction, while the other two in the opposite direction.

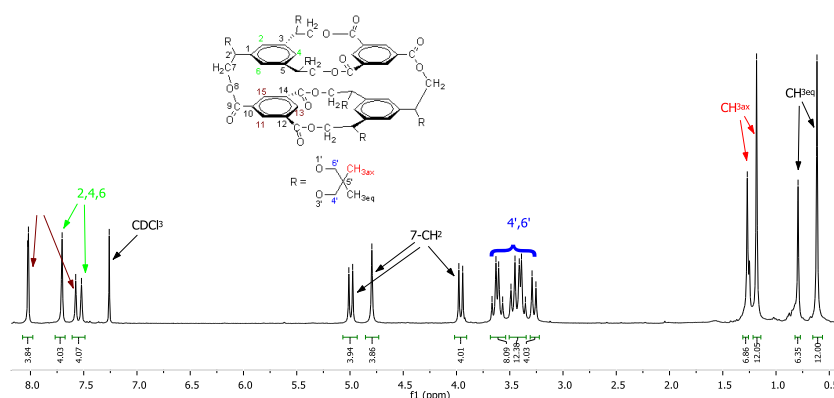
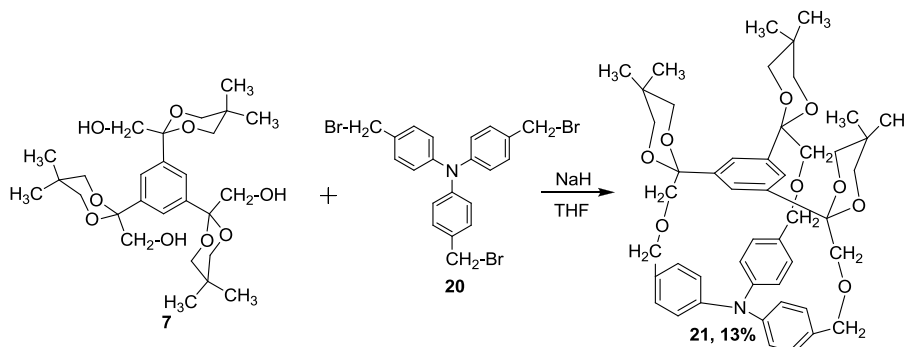


**Figure 16.**  $^1\text{H}$ NMR spectrum (300 MHz,  $\text{CDCl}_3$ ) of compound **15**

The reaction between trisbrominated derivative **20** and the trisdioxanic compound **7** was accomplished by ultra dilution technique, using THF as solvent and NaH as a base (**Scheme 16**). The major product of this reaction was the molecular cage **21**, which was isolated and fully characterized by means of NMR and MS spectra.



**Scheme 16**

The purification of this new cage proved to be very difficult requiring several chromatographic columns and the clean compound was obtained after HPLC separation. In spite of this, after purification the  $^1\text{H}$ NMR spectrum of the molecule reveals the expected number of resonances confirming this way the designed structure. In the aliphatic area we see two singlet signals corresponding to the equatorial and axial protons of the methyl group (0.62 ppm for  $\text{CH}_{3\text{eq}}$ , 1.29 ppm for  $\text{CH}_{3\text{ax}}$  respectively). A singlet signal is observed for  $\text{CH}_2$  protons from position 9 (3.39 ppm), two doublet signals for axial and equatorial protons from position 4 and 6 of the 1,3-dioxanic rings (3.44 ppm for axial protons, 3.53 ppm for equatorial protons), a singlet for  $\text{CH}_2$  protons from position 7 (3.82 ppm). In the aromatic area we three signals like we expected (a doublet at 7.35 ppm for protons from positions

12 and 14, a singlet at 7.50 ppm corresponding to protons from positions 1, 3 and 5 and a doublet at 7.79 ppm for protons from positions 11 and 15) (**Figure 23**).

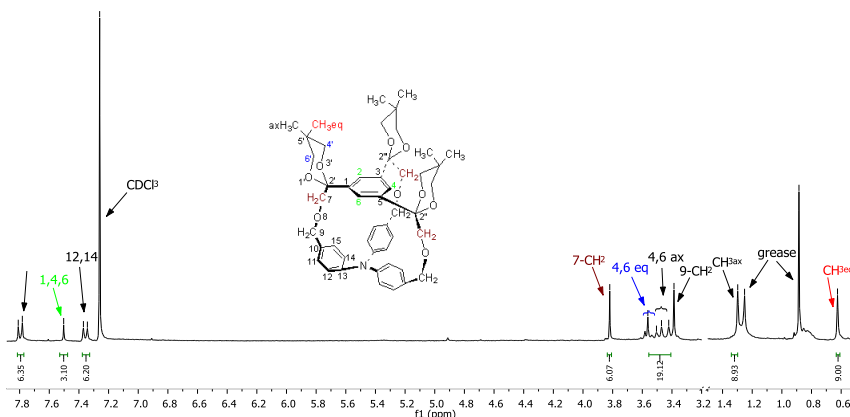
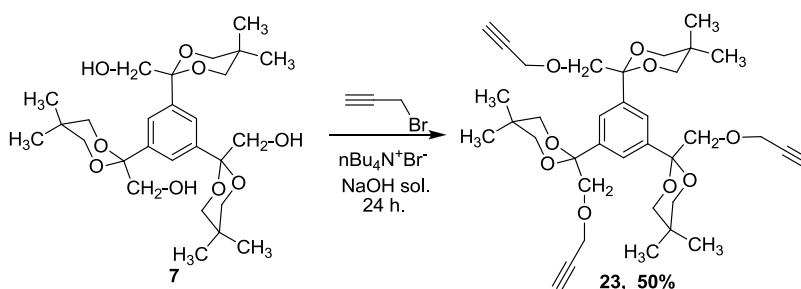


**Figure 23.**  $^1\text{H}$  NMR spectrum (300 MHz,  $\text{CDCl}_3$ ) of compound **21**

Compound **7** was involved in a phase transfer reaction with propargyl bromide, after a procedure adapted from literature,<sup>5,6</sup> in order to give a new compound (**23**), with a very good yield (**Scheme 18**).



**Scheme 18**

The structure of compound **23** was conformed by NMR and MS studies. The molecular structure of **23** (**Figure 26**) reveals similar aspects with those observed for **7**. The aromatic ring is axial for all 1,3-dioxane rings and two heterocycles are oriented in one side of the central aromatic unit, while the third 1,3-dioxane ring is oriented in opposite direction. The aromatic H atoms exhibit intramolecular contacts with the oxygen atoms of the heterocycles ( $d_{\text{O}\cdots\text{H}} = 2.488 - 2.564 \text{ \AA}$ ) and other  $\text{CH}\cdots\text{O}$  contacts with the 1,3-dioxane O atoms were observed for the H atoms of the  $\text{CH}_2\text{-O}$  units, too ( $d_{\text{O}\cdots\text{H}} = 2.342 - 2.564 \text{ \AA}$ ).

<sup>5</sup> Bogdan, N.D.; Matache, M.; Meier, V.M.; Dobrota, C.; Dumitru, I.; Roiban, G.D.; Funeriu, D.P., *Chem. Eur. J.*, **2010**, *16*, 2170.

<sup>6</sup> Wu, H.J.; Yen, C.H.; Chuang, C.T., *J. Org. Chem.*, **1998**, *63*, 5064-5070.

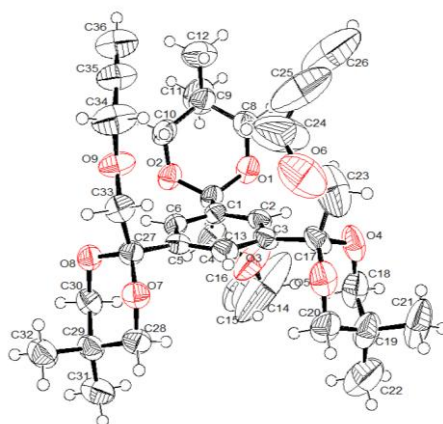


**Figure 26.** ORTEP diagram of compound **23**

The terminal H atoms of the propargyl groups play an important role in the building of the lattice. For each molecule, two propargyl groups form H-bondings with oxygen atoms belonging to heterocyclic units ( $d = 2.553 \text{ \AA}$ ) or to  $-\text{CH}_2\text{OCH}_2\text{C}\equiv\text{CH}$  groups ( $d = 2.656 \text{ \AA}$ ), while the third propargyl group is tilted towards an aromatic ring and exhibits C(sp)-H $\cdots\pi$  contact (the distance from the H atom to the centroid of the aromatic ring is  $d = 3.407 \text{ \AA}$ ) (**Figure 27**).

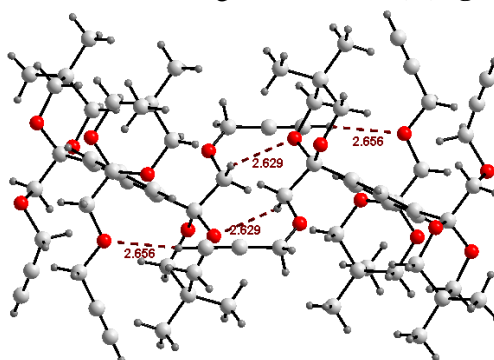
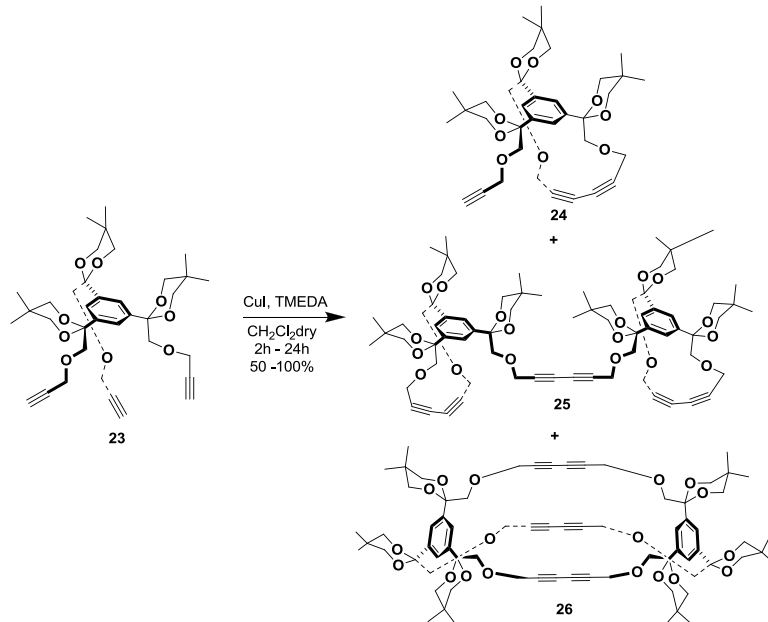


**Figure 27.** Diamond representation of the lattice showing the different intermolecular contacts

Acetylene coupling reaction was performed for our derivative with acetylene terminal groups (**23**). The oxidative coupling reactions were performed in Hay's conditions,<sup>7</sup> in dichloromethane, using CuI and tetramethylethylenediamine (TMEDA) as catalyst. The crude of the reaction afforded a mixture of three homocoupled products (**Scheme 19**). The three compounds were obtained in a

<sup>7</sup> Hamilton, D.G.; Prodi, L.; Feeder, N.; Sanders, J.K.M., *J. Chem. Soc., Perkin Trans 1*, **1999**, 1057-1065.

2:1:1 ratio with 50%, 25% and 25% yields, and they could be separated by column chromatography using as eluent ethyl acetate: pentane = 1:2.



**Scheme 19**

The NMR spectra of the three isolated compounds are different because of the magnetic nonequivalence of the protons belonging to the two types of branches. Molecular structure (**Figure 31**) of compound **24** reveals the molecule that we had designed, where two of the arms are intramolecularly connected while the third one is free.

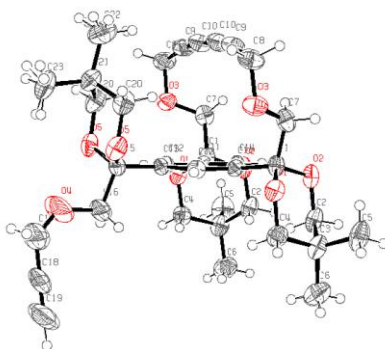


**Figure 31.** ORTEP diagram of compound **24**

<sup>1</sup>H NMR spectrum (**Figure 32**) of bis-macrocyclic **25** displays two sets of signals for the protons corresponding to the two types of branches, with an integration rapport of 2/1. We have singlet signals for protons from CH<sub>3eq</sub> and CH<sub>3ax</sub>. The

protons of positions 4 and 6 of the 1,3-dioxanic rings appear as a broad singlet at 3.46 ppm.

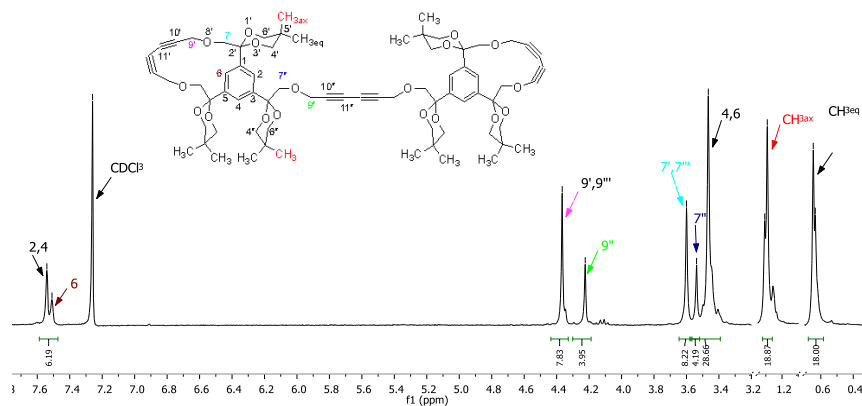


**Figure 32.**  $^1\text{H}$  NMR spectrum (300 MHz,  $\text{CDCl}_3$ ) of compound **25**

$^{13}\text{C}$  NMR spectrum (**Figure 34**) confirms the proposed structure displaying eleven types of signals corresponding to the eleven types of carbon atoms in the molecule, in agreement with a symmetrical structure.

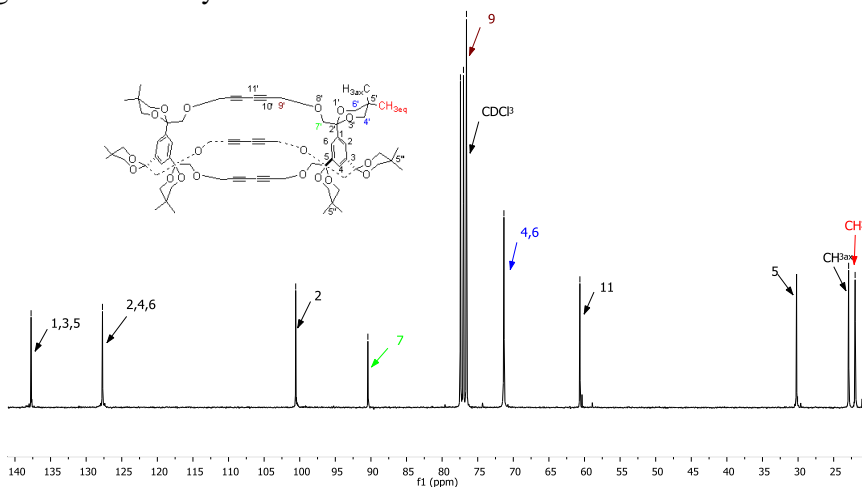
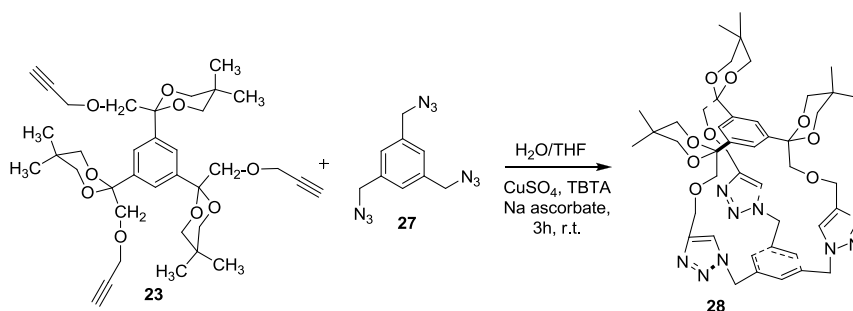


**Figure 34.**  $^{13}\text{C}$  NMR spectrum (75 MHz,  $\text{CDCl}_3$ ) of compound **26**

A subject of actuality in the field of supramolecular chemistry is the “click” reactions. We have proceeded to a click reaction between compound **23** and the triazide **27** conforming to **Scheme 21**, following a procedure adapted from the literature.<sup>8</sup> The reaction takes place in THF/ $\text{H}_2\text{O}$  as solvent,  $\text{CuSO}_4$ , hydrosoluble form of TBTA/sodium ascorbate<sup>9</sup> as catalyst.

<sup>8</sup> Karsten, S.; Ameen, M.A.; Kallane, S.I.; Nan, A.; Turcu, R.; Liebscher, J., *Synthesis*, **2010**, *17*, 3021-3028.



Scheme 21

The macrocycle **28** was analyzed by means of NMR spectroscopy and MS spectrometry and indeed the structure was confirmed. In the proton NMR spectrum of the compound we identified the expected number of resonances. In the carbon NMR spectrum as well, we find the expected number of resonances (**Figure 37**).

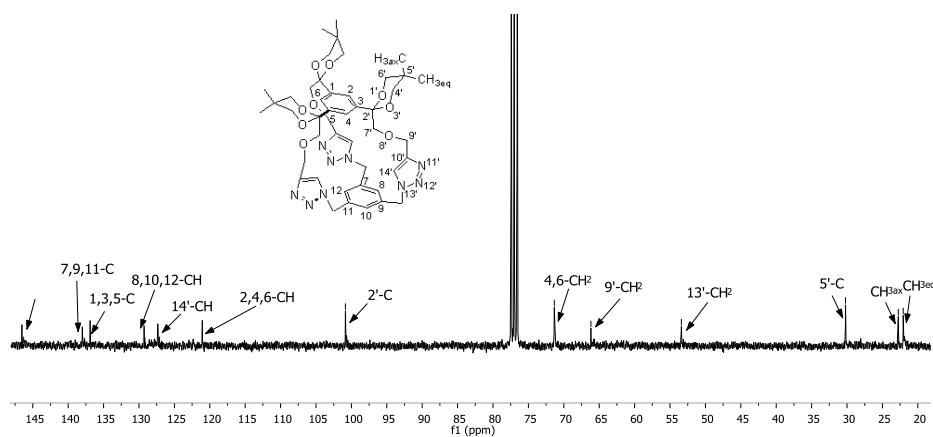


Figure 37.  $^{13}\text{C}$  NMR spectrum ( $\text{CDCl}_3$ , 75 MHz) of compound **28**

<sup>9</sup> Maisonial, A.; Serafin, P.; Traikia, M.; Debiton, E.; They, V.; Aitken, D.J.; Lemoine, P.; Viossat, B.; Gautier, A., *Eur. J. Inorg. Chem.*, **2008**, 298-305.

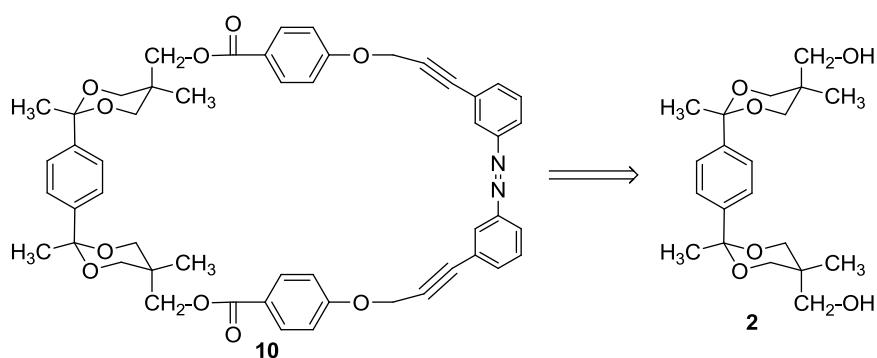
## **1.6. CONCLUSIONS**

- ◇ Starting from commercially available 4,4-dimethoxy-2-butanone one new trisubstituted aromatic building block with  $C_3$  symmetry (**7**) was synthesized.
- ◇ Derivatization of the trihydroxy derivative **7** by reaction with propargyl bromide, adapting a procedure reported in literature, led to a new tripodand with terminal triple bonds (**23**). Compound **23** was first described in this thesis.
- ◇ Different macrocyclization techniques were used to synthesize five new cage molecules (**11**, **14**, **15**, **16** and **21**) which were characterized by monodimensional and bidimensional NMR spectroscopy, mass spectrometry and X-ray diffraction analysis.
- ◇ Oxidative coupling reaction, performed in Hay's conditions, allowed the obtaining of three new macrocyclic compounds (**24**, **25** and **26**) that were fully characterized.
- ◇ A new macrocycle (**28**) was obtained by click reaction, and characterized by means of NMR spectroscopy and mass spectrometry.

**PART 2. MOLECULAR MACHINES**

## 2.2. RESULTS AND DISCUSSIONS

The target compound in our project is compound **10** presented in the retrosynthetic **Scheme 1**.



**Scheme 1**

The introduction of a unit that can be conformationally modified, in between the rods ends opposite to the pedal represents a very new element. In this way the movement caused in the pedal will be transmitted, through a bridge, to this unit. Depending on the motion sent by the pedal to the rods, the unit will prefer the conformation with a smaller or larger opening between the groups that tighten the ends of rods. The proposed conformationally changeable unit has a 1,4-bis(1,3-dioxan-2-yl)benzenic rest and is connected to the rods at 5' and 5'' positions of the 1,3-dioxanic ring (**Figure 5**).

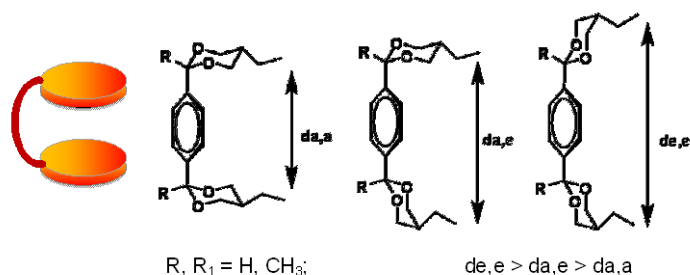
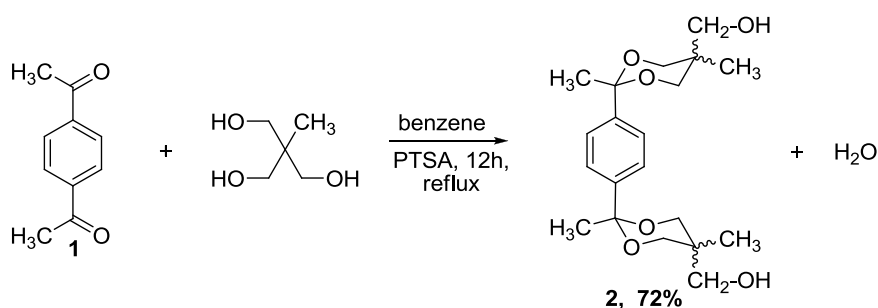


**Figure 5**

The distance between the ends of the dioxanic rings is small if the central benzenic ring is axial towards both dioxanic rings (axial-axial conformer), larger if one of the cycles is inverted and the aromatic unit has an axial-equatorial orientation and even larger if both dioxanic ring are inverted and the aromatic part is equatorial oriented toward both 1,3-dioxanic rings (equatorial-equatorial orientation). The energy differences between these conformers are relatively small and the inversion of 1,3-dioxanic rings can be induced by maneuvering the pedal (closing/opening). On the other hand these different conformers of the 1,3-dioxanic part are easily identified by NMR and these compounds allow an efficient and facile NMR monitoring of the molecular device.

The synthesis of the diastereomeric mixture of 1,4-(2,5,5-trimethyl-5,5-dihydroxymethyl-1,3-dioxan-2-yl)benzenes **2** (**Scheme 2**) was carried out following a previously described procedure.<sup>10,11</sup> In agreement with literature data (5, 15) the *trans-trans* isomer of **2** was indeed the major component (60%) of the above mixture as the *cis-trans* and *cis-cis* analogous were obtained in smaller amounts (**Figure 6**).

However, the separation of **2** could not be carried out neither by crystallization nor by column chromatography since the solubility of these diols in usual solvents was low. In addition, not only that the NMR spectra of the mixture **2** (c-c), **2** (c-t) and **2** (t-t) exhibited many non-separable signals but also their individual appearance was very similar.



**Scheme 2**

<sup>10</sup> Grosu, I.; Muntean, L.; Toupet, L.; Ple, G.; Pop, M.; Balog, M.; Mager, S.; Bogdan, E., *Monatsh. Chem.*, **2002**, *133*, 631.

<sup>11</sup> Balog, M.; Ph.D. Thesis, Babes-Bolyai University and Universite de Rouen, Cluj-Napoca, **2004**.

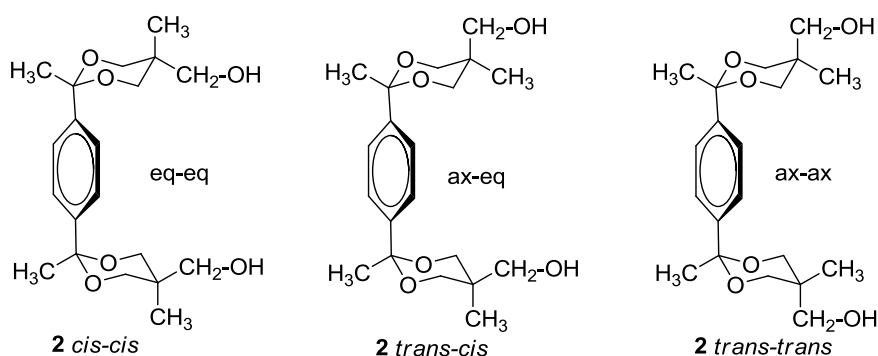
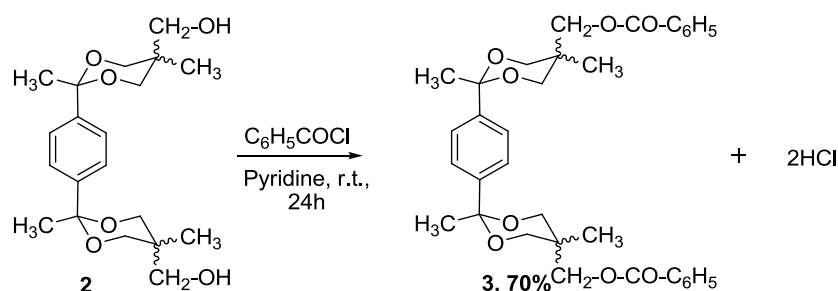


**Figure 6.** Stereoisomers representation of compound **2**

In order to avoid these problems, the mixture of stereoisomers of diol **2** was converted into the corresponding mixture of diesters upon benzylation with benzoyl chloride (**Scheme 3**).<sup>12</sup> The <sup>1</sup>H NMR signals of the new mixture of diastereomeric diesters were well separated allowing the individual assignment.

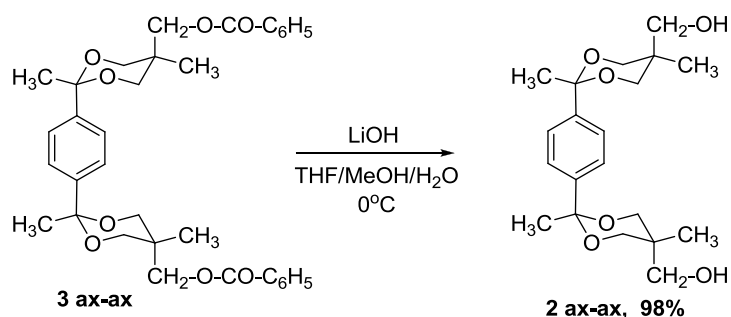


### Scheme 3

The axial-axial diester **3** could be isolated as single compound by column chromatography (eluent: ethyl acetate/petroleum ether 1:1) and we investigated it as unique structure. Then, by LiOH deprotection (**Scheme 4**) we succeed in obtaining the *trans-trans* diol **2** as a single compound. Its structure was fully confirmed by NMR and its molecular structure provided by X-ray diffractometry.<sup>13</sup>

<sup>12</sup> Balog, M.; Grosu, I.; Ple, G.; Ramondenc, Y.; Condamine, E.; Varga, R., *J. Org. Chem.*, **2004**, *69*, 137.

<sup>13</sup> Cîrcu, M.; Niste, V.; Varga, R.A.; Denes, E.; Bogdan, E.; Cismas, C.; Grosu, I., *Stud. Univ. Babeş-Bolyai Chem.*, **2010**, *3*, 183-190.



Scheme 4

The X-ray diffractometry molecular structure (**Figure 7**) revealed, as we expected, the axial orientation of the phenylene and hydroxymethyl groups together with the opposite orientation of the 1,3-dioxane rings with respect to the plane of the aromatic linker.

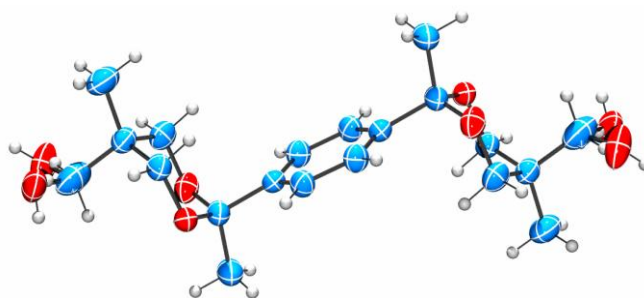


**Figure 7.** ORTEP diagram for the *trans-trans* diastereomer of **2**

In the lattice (**Figure 9**), the formation of linear polymers along the *c* axis by C-H $\cdots$  $\pi$  interactions involving the hydrogen atoms of the methyl groups at 1,3-dioxanic positions 2 and the aromatic rings were observed. Each aromatic unit is connected on both sides with the methyl groups of the neighboring molecules. The distance from the H atoms of the methyl group of one molecule to the centroid of aromatic ring of the partner molecule are  $d = 3.253, 3.648$  and  $3.714 \text{ \AA}$ .

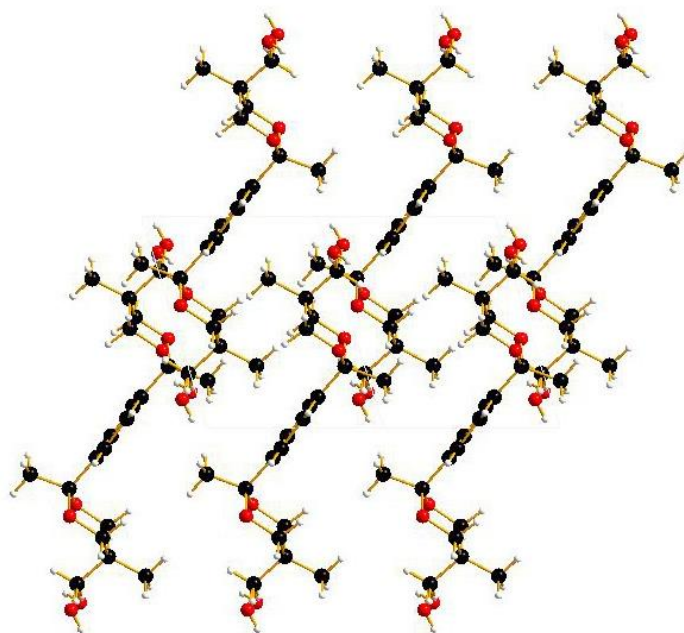


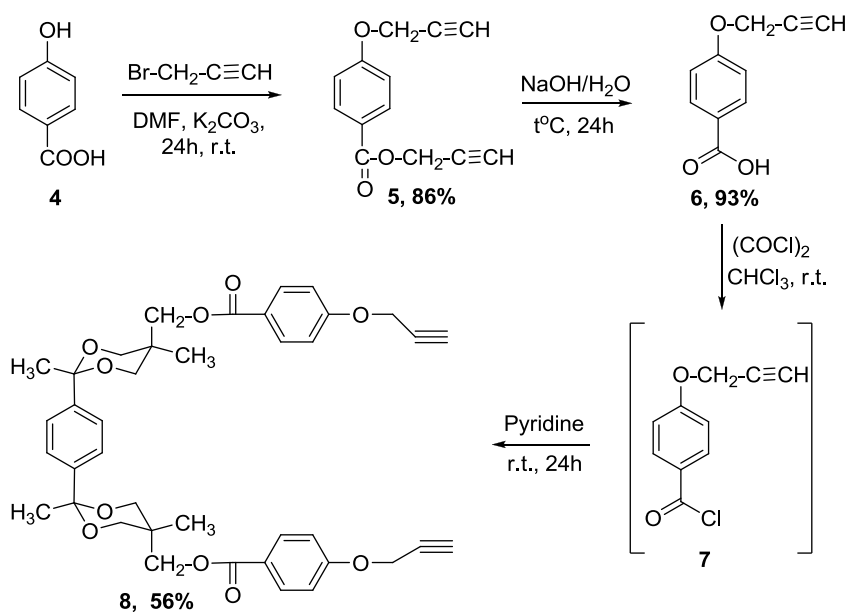
**Figure 9.** View (along the axis *c*) of the lattice of **2** (*trans-trans*)

In order to obtain the target molecule **8** we followed a reaction chain starting from commercially available 4-hydroxybenzoic acid (**4**), conforming to **Scheme 5**. The obtaining of compound **5** was achieved conforming to the literature data,<sup>14</sup> using 4-hydroxybenzoic acid, propargyl bromide, DMF as a solvent and potassium carbonate as a base. The product was confirmed by NMR and its structure is in agreement with the reported data. The next step in our work it was to synthesize derivative **6** as described in the literature.<sup>15</sup> Same as in the previous case, the structure of the compound was confirmed by NMR spectra. Compound **7** was synthesized starting from derivative **6**, which was reacted with oxalyl chloride in chloroform as the solvent. The reaction took place at room temperature and, for instability reasons, the product (**7**) was not isolated but used right away in the next reaction step for obtaining the key intermediate **8** with a good yield.

---

<sup>14</sup> Kanamathareddy, S.; Gutsche, C.D., *J. Org. Chem.*, **1996**, *61*, 2511-2516.

<sup>15</sup> Ramirez, C.; Beristain, M.F.; Ogawa, T., *Designed Monomers and Polymers*, **2004**, *7* (1-2), 85-99.



Scheme 5

All the intermediate derivatives were analyzed by means of NMR spectroscopy and MS spectrometry. The key intermediate **8** presents in the proton NMR spectrum the expected number of resonances. In the aliphatic area we can see two singlet signals corresponding to the protons of the methyl groups, 0.69 ppm for CH<sub>3</sub> protons from position 5' and 1.53 ppm for the CH<sub>3</sub> protons from position 2'. Then the triplet corresponding to the proton from position 19 is present at 2.57 ppm. Two doublet signals are observed for the protons from positions 4' and 6' of the 1,3-dioxanic ring (3.50 ppm for the axial protons, 3.72 ppm for the equatorial protons). The protons from the two different CH<sub>2</sub> groups resonance as singlet signals at 4.59 ppm and 4.79 ppm respectively. In the aromatic area we have a doublet signal for the aromatic protons from positions 11 and 15 (7.07 ppm), a singlet corresponding to the protons from positions 2, 3, 5 and 6 at 7.43 ppm, and a doublet corresponding to the protons from positions 12 and 14 (8.12 ppm) (**Figure 10**).

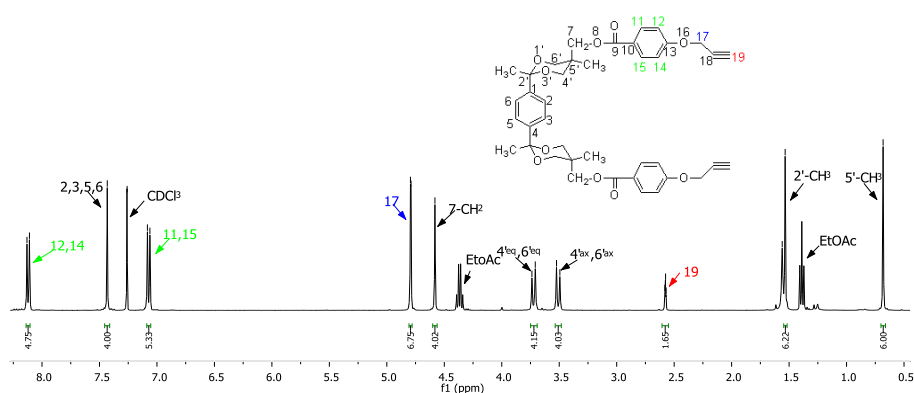
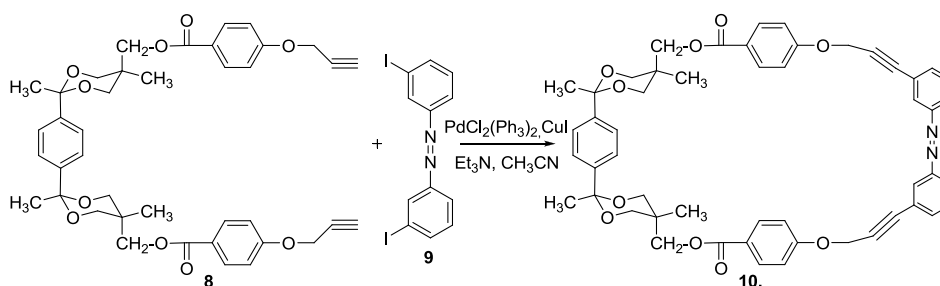


**Figure 10.**  $^1\text{H}$  NMR spectrum ( $\text{CDCl}_3$ , 300 MHz) of compound **8**

In order to achieve the target product **10** we submitted the intermediate **8** to a Sonogashira coupling reaction with diazo derivative **9** conforming to **Scheme 6**. The reaction was performed in anhydrous acetonitrile, using a Palladium catalyst and triethylamine as the base.



**Scheme 6**

The crude product of this reaction was purified on column chromatography and analyzed by NMR spectroscopy. Unfortunately the attribution of the signals was not possible due to the complexity of resonances present both in the  $^1\text{H}$  NMR and  $^{13}\text{C}$  NMR spectra. Nevertheless this project is still on going and we are optimistic that we will be able to achieve our goal of obtaining the desired product and study its activity.

## 2.3. CONCLUSIONS

◇ The synthesis of the diastereomeric mixture of 1,4-(2,5,5-trimethyl-5,5-dihydroxymethyl-1,3-dioxan-2-yl)benzenes **2** was carried out following a previously described procedure.

◇ The obtaining of the *trans-trans* diol **2** as a single compound was succeeded by LiOH deprotection reaction. Its structure was fully confirmed by NMR spectroscopy and its molecular structure provided by X-ray diffractometry.

◇ Starting from commercially available 4-hydroxybenzoic acid (**4**), following a multistep reaction procedure, one new disubstituted aromatic building block bearing 1,3,-dioxanic rings (**8**) was synthesized. Its structure was investigated by NMR spectroscopy and MS spectrometry.

◇ Sonogashira coupling reaction lead us to a new macrocyclic derivative (**10**) which was investigated by NMR spectroscopy but its structure was not yet determined.

◇ Nevertheless this project is still on going and we are optimistic that the structure of compound **10** is the one designed and we will be able to analyze its activity.

**PART 3. *BIOACTIVE SUGAR DERIVATIVES***



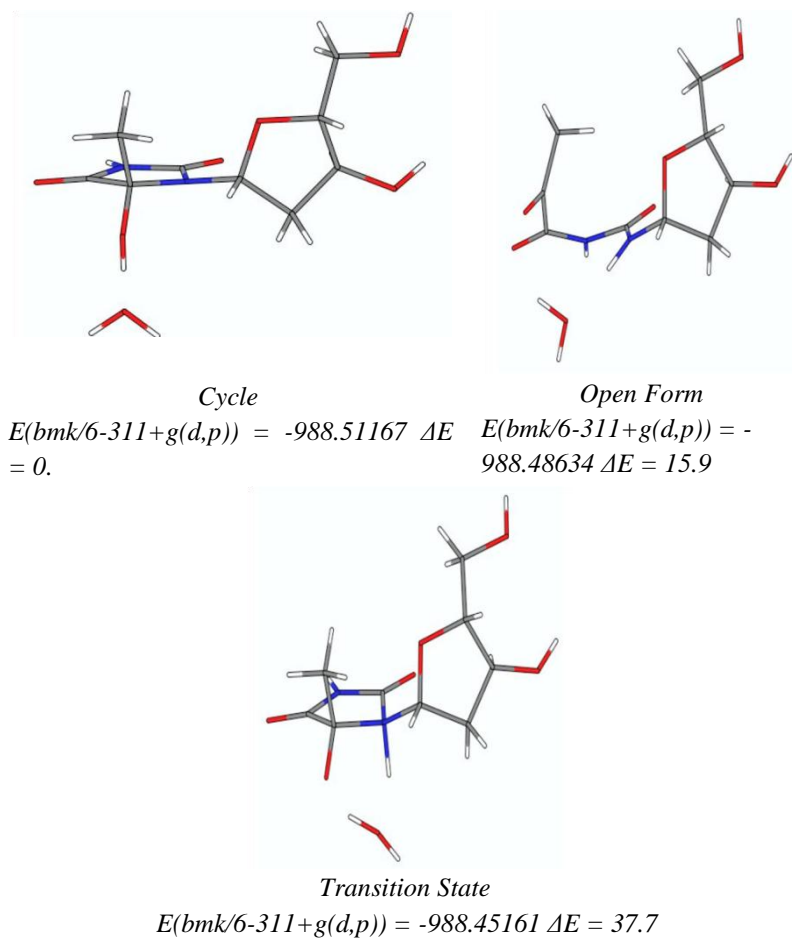


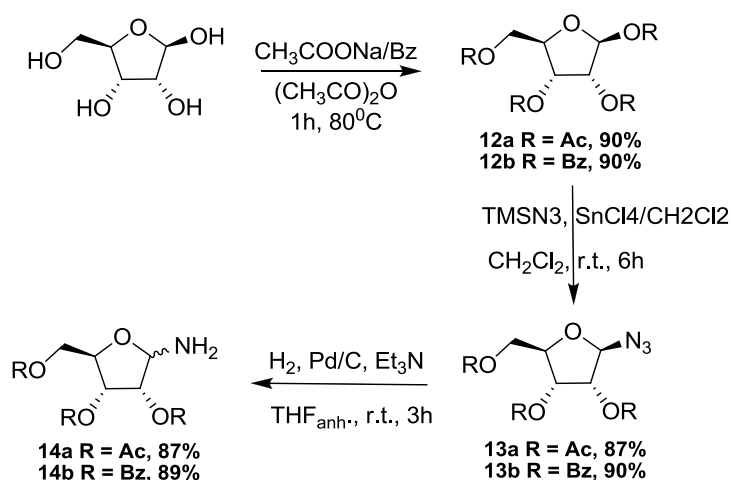
**Figure 1.** Theoretical calculations for hydantoin II

In a very recent paper<sup>17</sup> we have found structures similar with the ones we are interested in, where it is stated that this type of linear structures may be easily inserted into the active site of the repair enzymes. Also the presence of carbonyl and amino functions in the structure has shown to be involved in the recognition and the stabilization of the damaged DNA-protein repair complex.

In order to achieve the goal of this work we synthesize a series of compounds from which some are known and reported in the literature and others are new compounds. The first step was the protection of commercially available  $\beta$ -D-ribofuranose using the standard procedures. We conducted our work with both

<sup>17</sup> Gasparutto, D.; Muller, E.; Boiteux, S.; Cadet, J., *Biochimica et Biophysica Acta*, **2009**, 1790, 16-24.

acetyl and benzyl groups as protection groups for comparison reasons and also for convenience reasons, the benzyl protected derivatives being solid products that are easier to handle than the oily acetyl protected derivatives. The product of the protection reaction (1,2,3,5-tetra-O-acetyl- $\beta$ -D-ribofuranose **12a**, 1,2,3,5-tetra-O-benzoyl- $\beta$ -D-ribofuranose **12b**, respectively) was then submitted to a reaction with trimethylsilylazide in anhydrous dichloromethane<sup>18,19</sup> in order to obtain the  $\beta$ -D-ribofuranosyl azides **13a** and **13b**. These two azides were hydrogenated in anhydrous THF to afford the corresponding amines **14a**<sup>20</sup> and **14b** with very high yields (**Scheme 7**).



Scheme 7

From the NMR analysis we could deduce that compounds **12 (a,b)** and **13 (a,b)** are present as single compounds, while in the case of compound **14 (a,b)** the spectrum reveals the presence of both anomeric structure. Although at the first look we were tempted to affirm that we see in the NMR the amino derivative but also the unreacted azide, the TLC showed only one new spot, the spot corresponding to the starting material being absent. This made us think that we are not dealing with a mixture containing unreacted starting material and new compound, but with a mixture of anomers. The mass spectrum confirmed our theory presenting only one pick corresponding to the amino derivative (ESI+ ( $m/z$ ) = 276).

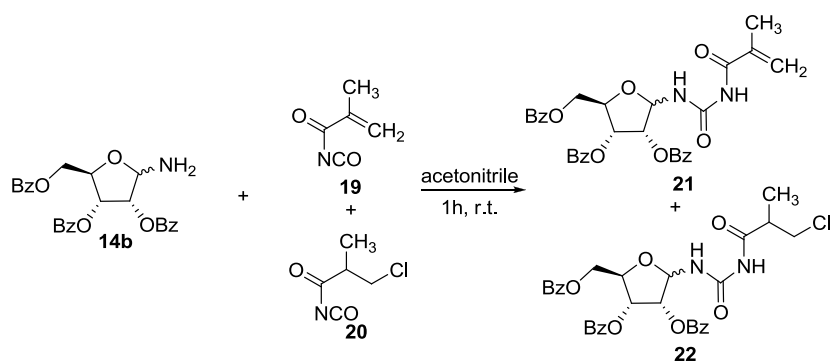
We submitted this mixture to the next step (**Scheme 10**) hoping that we will be able to separate the final urea products but this proved to be even more difficult because we obtained not only the expected ureas **21** and **22** but also their anomeric

<sup>18</sup> Stimac, A.; Kobe, J., *Carbohydrate Research*, **1992**, 232, 359-365.

<sup>19</sup> Camarasa, M.J.; Alonso, R.; de las Heras, F.G., *Carbohydrate Research*, **1980**, 83, 152-156.

<sup>20</sup> Ichikawa, Y.; Matsukawa, Y.; Nishiyama, T.; Isobe, M., *Eur. J. Org. Chem.*, **2004**, 586-591.

structures. In the NMR it was impossible to identify the compounds, the only prove that we had being the MS spectra where we can easily observe the picks corresponding to the two urea derivative desired (ESI+:  $m/z = 573$  for **21**, and  $m/z = 609$  for **22**).



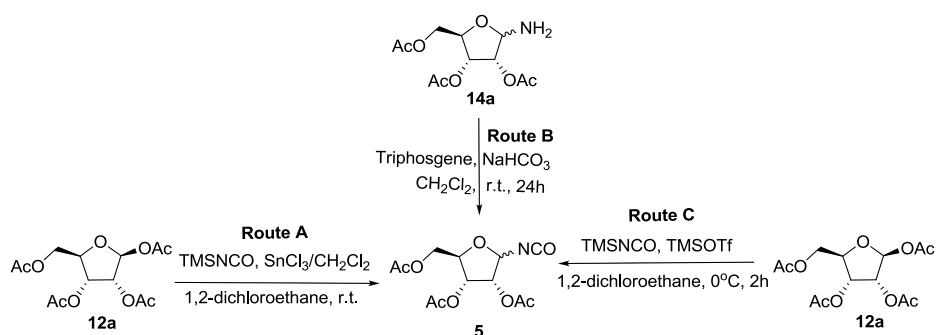
**Scheme 10**

Taking into consideration all the data that we had and the fact that even if we obtain the target compounds it is practically impossible to purify them, we decided to change the synthesis strategy. Instead of having the amine group on the ribofuranosyl ring and react it with the small isocyanate molecules, we thought of obtain the ribofuranosyl isocyanate (**5**) and react it with the pyruvamide **6**. In order to synthesize the ribofuranosylisocyanate **5** we have tried three different synthetic routes<sup>21,22,23</sup> (**Scheme 11**) and we choose route **C** as the most convenient one (the starting material is commercially available, the reaction time is reduced comparing to the other two routes and the reaction mixture does not need a work-up for the next step).

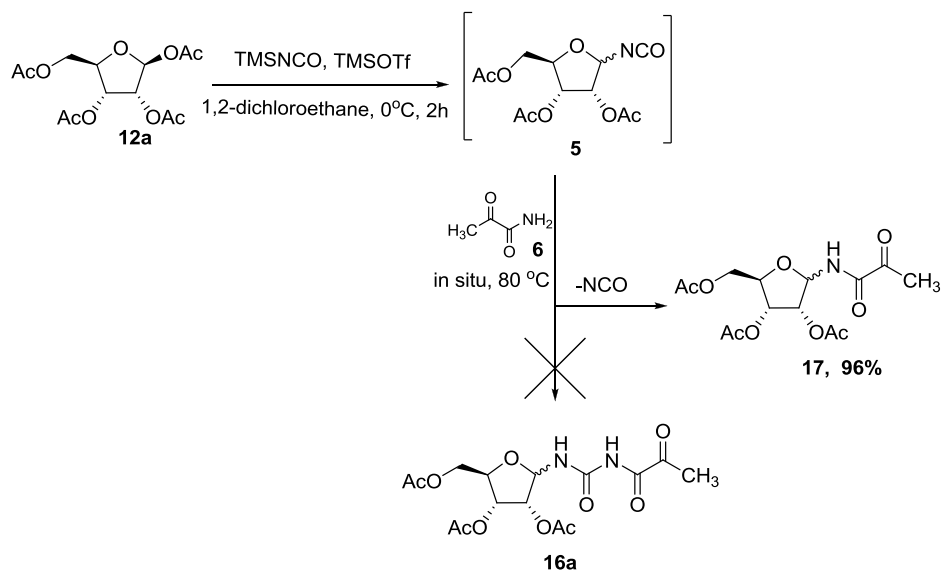
<sup>21</sup> Stimac, A.; Kobe, J., *Carbohydrate Research*, **1992**, 232, 359-365.

<sup>22</sup> Goody, R.S.; Jones, A.S.; Walker, R.T., *Tetrahedron*, **1971**, 27, 65-69.

<sup>23</sup> Haines, D.R.; Leonard, N.J.; Wiemer, D.F., *Journal of Organic Chemistry*, **1982**, 47, 474-482.



Next step was to proceed to the reaction between the compound **5** and pyruvamide **6**, in order to obtain the target urea **16**. We tried the reaction according to the literature<sup>24</sup> but at the end we didn't isolate the desired product, so we thought of adding the amide in situ (**Scheme 12**). The reaction proved to be a successfully one and we were able to isolate and analyze the product. This product that we obtained, under conditions developed in our laboratory, was initially assigned the structure of the open pyruvoyl-urea isomer **16a**, based on the <sup>1</sup>H and <sup>13</sup>C NMR. Discrepancies were nevertheless observed in the data of this derivative so after a better analysis it was found that **5** was a particularly unstable substance with the isocyanate group behaving as a good leaving group, leading to *N*-pyruvoyl- $\beta$ -D-ribofuranosylamine **17**.



<sup>24</sup> Oikonomakos, N.G., et al, *J. Med. Chem.*, **2005**, *48*, 6178-6193.

In the  $^1\text{H}$  and  $^{13}\text{C}$  NMR spectra of compound **17**, two species are observed with similar signals in a  $\approx 1:1$  ratio. They were assigned to the two conformers, due to the known impeded rotation of the amidic bond (N7-C8). In the proton NMR spectrum of compound **17** (**Figure 3**), the pick corresponding to the anomeric position appears as a multiplet (5.92-6.02 ppm) instead of a doublet of doublets like we would expect for a single compound. The same situation we observe in the aliphatic area where instead of a singlet corresponding to the protons from methyl group from position 12, we have two singlet signals (2.48, 2.49 ppm).

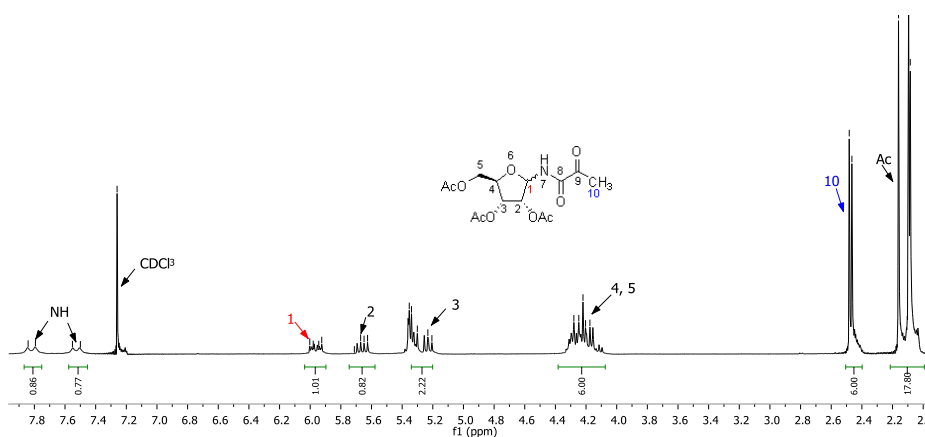


**Figure 3.**  $^1\text{H}$  NMR spectrum (200 MHz,  $\text{CDCl}_3$ ) of compound **17**

In **Figure 4** it is presented the carbon NMR spectrum of compound **17**. As it can be observed all the picks are doubled as corresponding to the two anomeric conformers proposed.

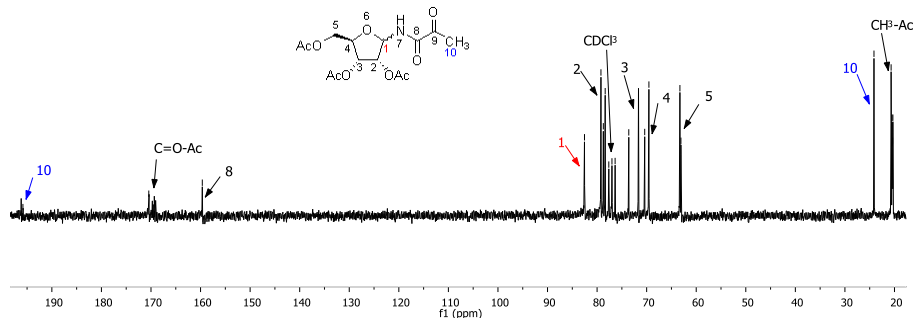
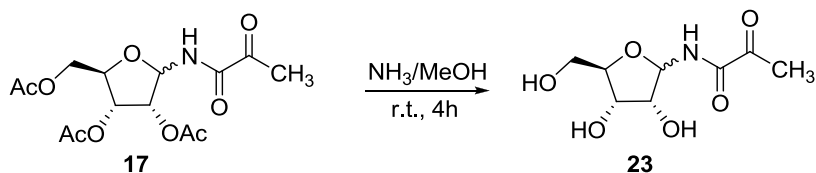


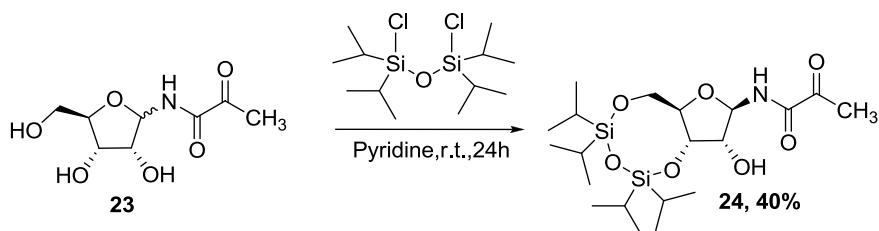
**Figure 4.**  $^{13}\text{C}$  NMR spectrum (50 MHz,  $\text{CDCl}_3$ ) of compound **17**

Compound **17** was submitted to a deprotection reaction with ammonia in methanol for 4 hours and the deprotected derivative **23** was obtained quantitatively also as a mixture of inseparable anomers (**Scheme 13**).



**Scheme 13**

Forcing the cyclization of the open structure by silylation (**Scheme 14**) to the closed structure we manage to block the anomerization and we obtained only the proposed derivative **24** as a single anomeric structure with a fair yield. The origin of this stereoselectivity is unclear, but in our opinion it is definitely related to the TIPDS protection.



**Scheme 14**

In **Figure 5** we have a depicted spectrum of compound **24**. As it can be observed the picks corresponding to the protons from the TIPDS groups (0.99 to 1.06 ppm) are of a very high intensity comparing with the rest of the protons from the molecule. The representative pick for the anomeric position 1 (5.75 ppm) appears as a doublet of doublets as expected for a single compound and not as multiplet like in the case before.

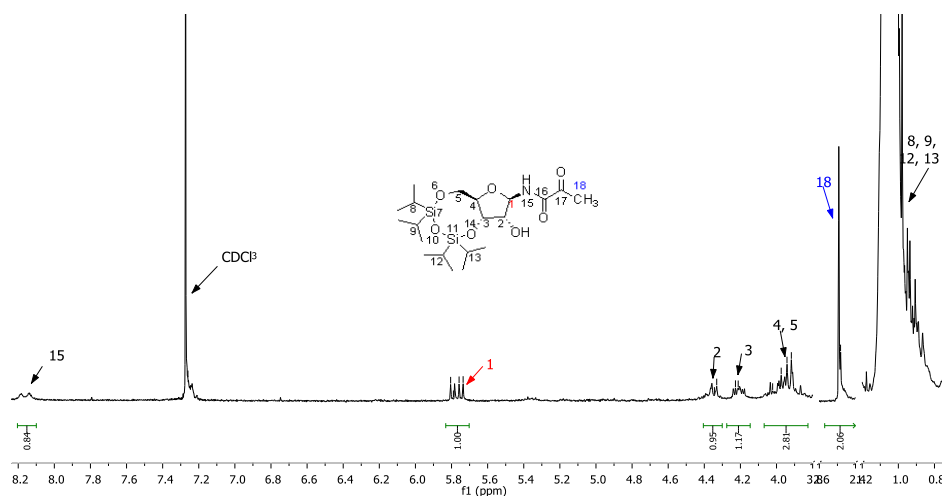


**Figure 5.**  $^1\text{H}$  NMR spectrum (200 MHz,  $\text{CDCl}_3$ ) of compound **24**

In  $^{13}\text{C}$  NMR (**Figure 6**) we can easily observe that, comparing to the compounds where we had a mixture of anomers, here the signals are not doubled. Thus, for the carbon from position 1 we have the peak at 80.43 ppm, for  $\text{C}_2$  we have a peak at 79.52 ppm, 72.70 ppm for  $\text{C}_3$ , 70.27 ppm for  $\text{C}_4$ , 62.25 ppm for  $\text{C}_5$ , respectively.

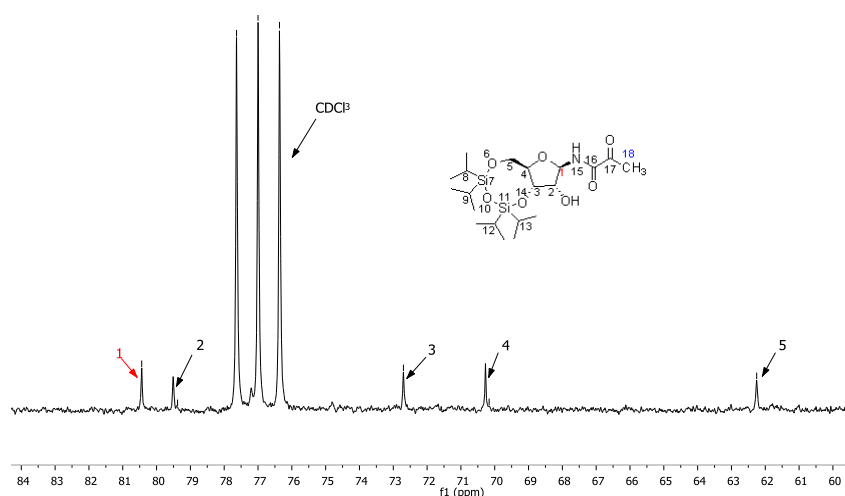
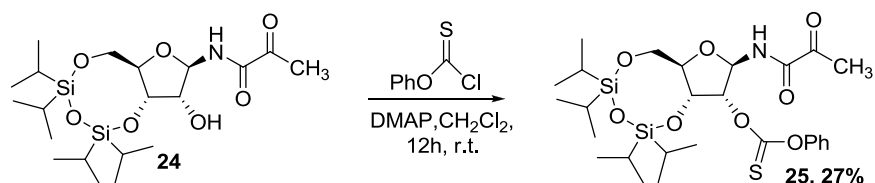


**Figure 6.**  $^{13}\text{C}$  NMR fragment (50 MHz,  $\text{CDCl}_3$ ) of compound **24**

Compound **24** was submitted to a 12 hours reaction in dichloromethane, in order to protect the free OH group from position 2 (**Scheme 15**). The product **25** was obtained with a good yield and the NMR shows the presence of a single compound.



**Scheme 15**

In the **Figure 7** it is presented a representative fragment from the  $^1\text{H}$  NMR spectrum and the  $^{13}\text{C}$  NMR spectrum of compound **25**. The picks corresponding to position 1 are as we expected doublet of doublets for proton (5.74 ppm) and a single pick for carbon (80.44 ppm). In the aromatic area we have the picks corresponding to the phenyl group (6.81-6.92 ppm for protons and 115.34 ppm for carbons from ortho-position of the phenyl group, 7.17-7.26 ppm for protons and 129.52 ppm for carbons from metha-position of the phenyl group).

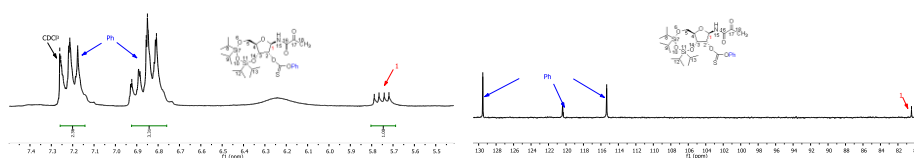
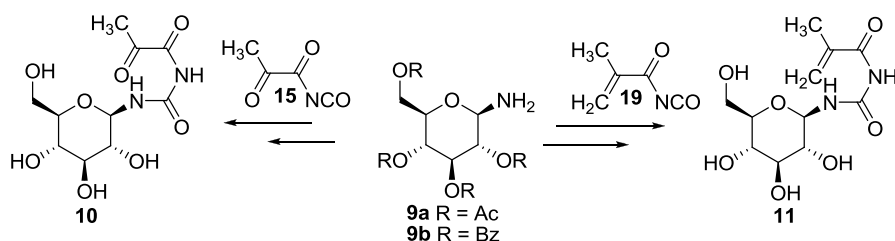


**Figure 7.**  $^1\text{H}$  NMR (200 MHz,  $\text{CDCl}_3$ ) and  $^{13}\text{C}$  NMR (50 MHz,  $\text{CDCl}_3$ ) fragments of compound **25**

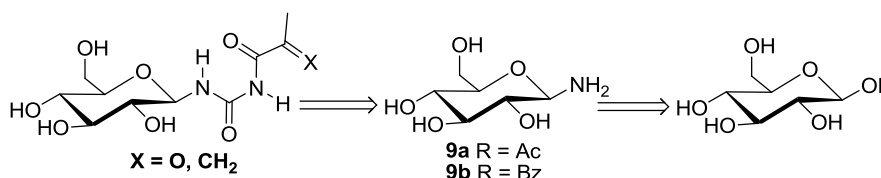
The chemistry was carried in parallel with  $\beta$ -D-glucopyranosyl derivatives (**Scheme 17**), in order to characterize all intermediates by protein crystallography (soaking of crystals of Glycogen Phosphorylase) and at the same time look for possible strong inhibitors of this enzyme.



**Scheme 17**

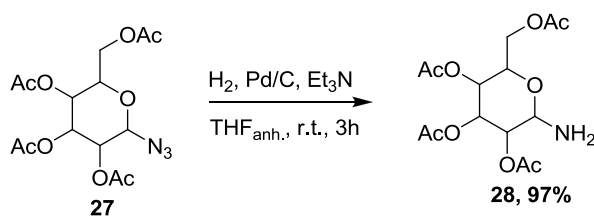
As I mentioned in the beginning of this chapter this project was conducted in parallel with the work on  $\beta$ -D-glucose correspondents. The synthetic strategy is

similar with the one in  $\beta$ -D-ribose case and the retrosynthetic scheme is presented below (**Scheme 18**).



**Scheme 18**

Having 5-Ac-glucopiranosil azide (**27**) as starting material, through a hydrogenation reaction,<sup>42</sup> we arrived to the desired amine **28** quantitatively (**Scheme 20**):



**Scheme 20**

Comparing with the ribofuranosyl derivatives case, all the intermediates of glucose, including the amine (**28**), were obtained as single compounds and not as mixture of anomers. For this reason the work-up, the purification and the analysis of this compounds could be accomplished much easier than in the previous case.

In the proton NMR spectrum of compound **28** we have 4 singlet signals (2.00-2.08 ppm) corresponding to the protons of CH<sub>3</sub>-Ac groups, a ddd pick (at 3.68 ppm) for H<sub>5</sub>, two dd signals (4.09 ppm, 4.21 ppm respectively) for CH<sub>2</sub>-6, singlet signal for H<sub>1</sub> and three triplet signals for H<sub>2</sub>, H<sub>4</sub>, H<sub>3</sub> at 4.81, 5.03 and 5.23 ppm (**Figure 8**).

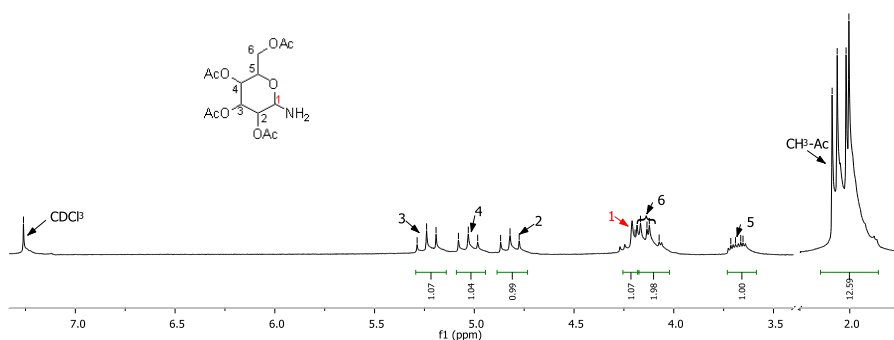


**Figure 8.**  $^1\text{H}$  NMR spectrum (200 MHz,  $\text{CDCl}_3$ ) of compound **28**

In **Figure 9** it is presented the carbon NMR spectrum of compound **28** where again we see the presence of a single compound.

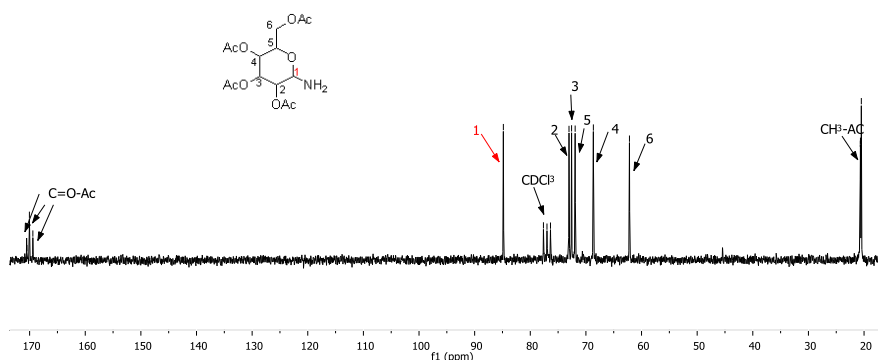
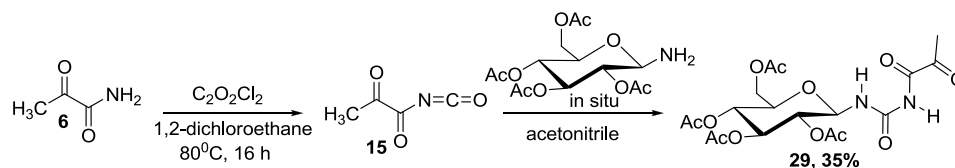


**Figure 9.**  $^{13}\text{C}$  NMR spectrum (50 MHz,  $\text{CDCl}_3$ ) of compound **28**

Pyruvamide (**6**) was submitted to a 2 steep, but one pot, reaction in order to obtain the desired derivative **29** (N-( $\beta$ -D-glucopyranosylcarbamoyl)pyruvamide) conforming to **Scheme 19**. The isocyanate derivative **15** was not isolated and the second reactant was added in situ for the second step of the reaction. The experimental procedures for similar compounds described in literature<sup>25</sup> were modified and are described in the experimental procedure. In this case the reaction lead us to the product expected, the NCO group from the small linear structure **15** proving not to be such a good living group like in the case when situated on the sugar ring.

<sup>25</sup> Oikonomakos, N.G., et all, *J. Med. Chem.*, **2005**, *48*, 6178-6193.



**Scheme 19**

The product was analyzed by means of NMR and MS spectra and proves to be the linear structure that we designed. Although in the proton NMR spectrum we could observe the appearance of a new signal, corresponding to the new CH<sub>3</sub> group, the <sup>13</sup>C NMR is the best prove that our structure is the one we desired. Thus, comparing with the starting material, in the products spectrum we have four new picks: δ(ppm): 24.12 for 13-CH<sub>3</sub>, 159.11 for 9-CO, 162.26 for 11-CO, and 196.58 for 12-CO (**Figure 10**).

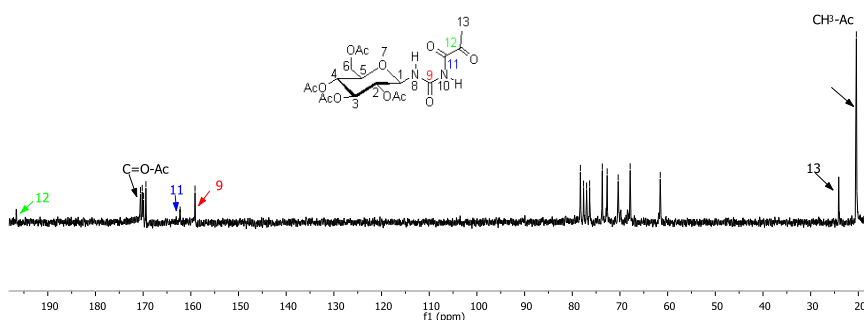
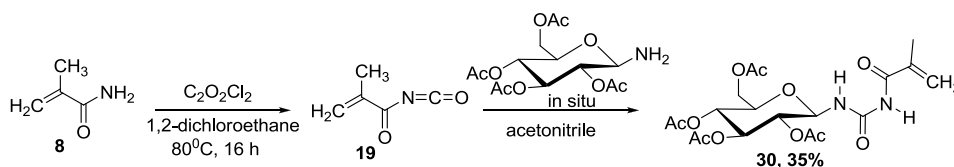


**Figure 10.** <sup>13</sup>C NMR spectrum (50 MHz, CDCl<sub>3</sub>) of compound **29**

Methacrylamide (**8**) is the starting material for the obtaining of another urea derivative (**30**, N-(β-D-glycopyranosylcarbamoyl)methacrylamide). The reaction scheme is represented in **Scheme 21**.



**Scheme 21**

In the <sup>1</sup>H NMR spectrum of this new compound we have the characteristic pick as a singlet at 2.08 ppm for CH<sub>3</sub> protons, and two broad singlet signals (5.61 ppm, 5.90 ppm respectively) for the two protons of the CH<sub>2</sub> group. The <sup>13</sup>C NMR

spectrum contains five new signals:  $\delta$  (ppm): 20.57 for 13-CH<sub>3</sub>, 123.76 for 12-CH<sub>2</sub>, 138.26 for 12-C, 154.22 for 9-CO and 168.61 for 11-CO (**Figure 11**).

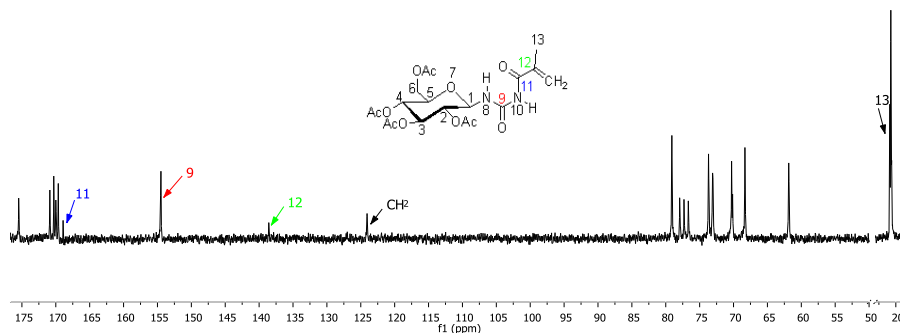
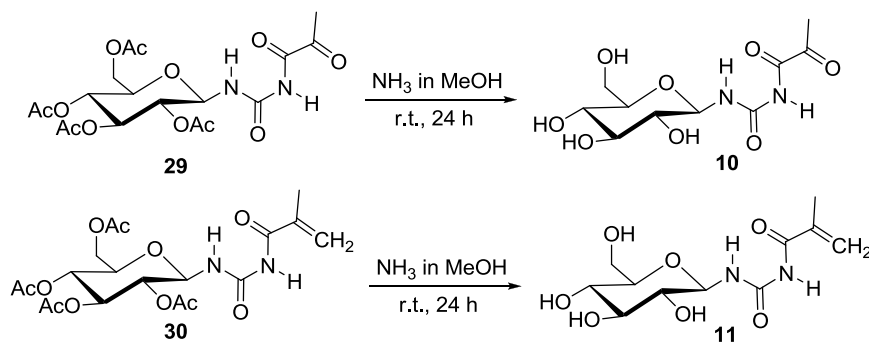


**Figure 11.** <sup>13</sup>C NMR spectrum (50 MHz, CDCl<sub>3</sub>) of compound **30**

Both urea derivatives obtained (**29** and **30**) were submitted to deprotection reactions, with ammonia in methanol at room temperature, in order to arrive to the desired structures **10** and **11**, conforming to **Scheme 22**.



**Scheme 22**

The target molecules **10** and **11** will be tested as possible inhibitors for Glycogen Phosphorylase by soaking of the crystals on this enzyme.

### **3.3. CONCLUSIONS**

- ◇ Starting from commercially available  $\beta$ -D-ribofuranose and  $\beta$ -D-glucose a series of new compounds (**10**, **11**, **17**, **23**, **24**, **25**, **30**, **32**) were obtained.
- ◇ We have accomplished the key step coupling reaction by using a protected ribosylamine isocyanate (**5**), prepared by a new methodology (TMSNCO, TMSOTf, DCE, 0°C) and readily prepared pyruvamide (**6**), in a one-pot reaction.
- ◇ Although both anomers for the ribofuranosyl derivatives were obtained, the beta anomer could be isolated in pure form after TIPDS protection and it appears configurationally stable.
- ◇ The lack of any spontaneous cyclization of the open structure to the 5-hydroxyl-5-methyl-hydantoin lesion indicates that the open structure is biologically relevant and its mutation potential should be studied in detail.
- ◇ Two new  $\beta$ -D-glucopyranosyl derivatives protected with acetate groups (**30**, **32**) were obtained and their deprotected forms (**10**, **11**) will be tested as biological active compounds.